Comparison among different sintering routes for preparing alumina-YAG nanocomposites

Paola Palmero[a,*], Antonia Simone[a], Claude Esnouf[b],
Gilbert Fantozzi[b], Laura Montanaro[a]

[a] *Department Materials Science and Chemical Engineering, Politecnico di Torino, INSTM Research Unit (LINCE Lab),
Corso Duca degli Abruzzi, 24-10129 Torino, Italy*
[b] *GEMPPM, INSA de Lyon, 20 Av. A. Einstein, 69621 Villeurbanne, France*

Abstract

Al_2O_3-YAG (50 vol.%) nanocomposite powders were prepared by wet-chemical synthesis and characterized by DTA-TG, XRD and TEM analyses. Amorphous powders were pre-heated at different temperatures (namely 600 °C, 800 °C, 900 °C and 1215 °C) and the influence of this thermal treatment on sintering behavior, final microstructure and density was investigated. The best performing sample was that pre-calcined at 900 °C, which yields dense bodies with a micronic/slightly sub-micronic microstructure after sintering at 1600 °C. A pre-treatment step to induce controlled crystallisation of the amorphous powder as well as a fast sintering procedure for green compacts, were also performed as a comparison.

Finally, the previously stated thermal pre-treatment of the amorphous product was coupled to an extensive mechanical activation performed by wet planetary/ball milling. This procedure was highly effective in lowering the densification temperature, so that fully dense Al_2O_3-YAG composites, with a mean grain size smaller than 200 nm, were obtained by sintering in the temperature range 1370–1420 °C.

1. Introduction

Many works have been devoted to the manufacturing of nanostructured ceramics over the past 15 years, and some recent reviews [1,2] have clearly reported the state-of-the-art as well as the expected progress in producing fully dense ceramic nanostructures. Some approaches in limiting grain coarsening during densification seem to be successful. The first one is the use of particular consolidation techniques (such as hot isostatic pressing, spark plasma sintering, microwave sintering, . . .) instead of natural sintering.[1,2] The second way consists in the addition of dopants, able to limit grain boundary migration (for instance, by a "pinning" effect), and hence

grain growth.[3] Finally, when metastable phases are present in the starting green body, densification can be enhanced at a lower sintering temperature by a pre-seeding with the final stable phase.[4,5] In addition, it has been recently[6] demonstrated that it is possible to manufacture nanostructured ceramics by using a normal sintering practice, just divided in two steps ("*two-step sintering*"), thereby exploiting the difference in kinetics between grain boundary diffusion and grain boundary migration. Another processing route successfully tested is the so-called *fast sintering*, which can provide high final density, without associated grain growth.[7–9] It generally involves a fast soaking of the specimen into a pre-heated furnace at high temperature for a shorter time than in conventional sintering. Some more conventional approaches to nanosintering, however, have limits when composite materials must be densified, due to the differences in diffusion mech-

* Corresponding author. Tel.: +39 011564700; fax: +39 0115644665.
E-mail address: paola.palmero@polito.it (P. Palmero).

anisms and densification/coarsening temperatures of the two or more phases involved. Among oxide-based nanocomposites, the alumina-based ones have been recently recognised[10] as one of the most difficult to produce, since alumina possesses a very high homologous temperature for full-density sintering and can undergo several phase transformations during consolidation when transition alumina is used as starting material. In the same paper, conventional processing routes (such as pressureless sintering) have failed to yield dense nanostructured materials.

In the case of alumina-yttrium iron garnet (YAG) materials some promising results in maintaining the nanoscale of the composite material have been obtained by using non-conventional sintering routes[11].

This paper deals with an alumina-YAG amorphous powder obtained by a wet chemical route and with attempts to densify it as a nanoscaled material by using conventional sintering routes coupled to particular mechanical and/or thermal powder pre-treatments. The results of a fast sintering procedure are also reported.

2. Experimental procedure

An alumina-YAG composite powder having a 50 vol.% composition (AY50) has been synthesised at $25\,^{\circ}$C by inverse co-precipitation, using the so-called *reverse-strike* method[12–14], that is adding (at the rate of 10 ml/min) the aqueous solution of the two metal chlorides (0.33 M $AlCl_3 \cdot 6H_2O$ and 0.064 M $YCl_3 \cdot 6H_2O$) to an ammonia solution (8 M), kept at a constant pH of 9 (± 0.2) during precipitation, by extra-ammonia solution (16 M) addition. The gelatinous precipitate was filtered on a sintered-glass filter and washed four times by dispersing the filtered cake in dilute ammonia (1 g of filtered precipitate/1 ml of 8 M ammonia solution), for eliminating the precipitation by-products, and then twice with absolute ethanol (maintaining the above "precipitate weight /liquid volume" ratio), for limiting hard agglomeration during drying. The dried powder was wet-planetary milled (with agate balls in an agate vessel) in absolute ethanol for 4 h and then characterised by simultaneous DTA-TG (Netzsch STA 409C). The phase evolution as a function of temperature was studied by X-ray diffraction (XRD, Philips PW 1710). The crystallite formation and size were investigated by TEM (Jeol 200 CX) analyses performed on powders calcined in air, in the temperature range between 900 and $1300\,^{\circ}$C, for a soaking time of 30 min.

From the above results, powder samples were thermally pre-treated at various temperatures (heating and cooling rate of $10\,^{\circ}$C/min), as detailed below. Bars were then uniaxially pressed at 300 MPa and sintered inside a dilatometer (Netzsch 402E), in static air, at $1600\,^{\circ}$C for 3 h (heating and cooling rate of $10\,^{\circ}$C/min), to reach full densification. Some powder samples were also added with 500 ppm MgO[15,16] and then pressed and sintered in the same conditions.

Pellets of powders pre-treated at $900\,^{\circ}$C for 30 min were also submitted to a *fast sintering* which includes a rapid heating step ($50\,^{\circ}$C/min) to $1600\,^{\circ}$C, an isothermal step at the maximum temperature for 18 min and cooling down to room temperature at $20\,^{\circ}$C/min, following literature indications[9].

A thermal pre-treatment to induce partial crystallisation of the two final phases was also carried out by plunging the amorphous powder into a vertical furnace kept at $1290\,^{\circ}$C, at which both YAG and α-alumina crystallize, for a time ranging from 0 to 15 min. After that, the powders were pressed and sintered in a dilatometer, following the previously described procedure.

Finally, some of the above pre-treated powders underwent an extensive mechanical activation prior to compaction and natural sintering. A wet planetary grinding was performed in absolute ethanol for two hours by using agate vessels and balls (1 cm in diameter) followed by a wet ball milling for 30 h by using a polymeric vessel and ceramic (alumina or zirconia) or polymeric (polyethylene) balls (0.25 cm in diameter). An Italian patent has been recently deposited on this procedure.[17] XRD and BET analyses were performed on the powdered materials before and after such milling procedure.

3. Results and discussions

DTA performed on the amorphous precipitate showed three exotherms at about $980\,^{\circ}$C, $1120\,^{\circ}$C and $1215\,^{\circ}$C, respectively. The first peak was associated to the crystallization of a hexagonal, metastable phase (h-$YAlO_3$).[18] The higher temperature peaks were imputed to the crystallization of the stable phases, which are YAG and α-alumina respectively, on the ground of XRD analyses.

The crystallite size as a function of the temperature was investigated by TEM observations in dark field. At $900\,^{\circ}$C for 30 min the hexagonal phase presented a mean grain size of about 20 nm (Fig. 1a), while after calcination at $1300\,^{\circ}$C for 30 min, the YAG and α-Al_2O_3 crystallites reached a mean size of about 120 nm (Fig. 1b). In Fig. 2 the crystallite size evolution as a function of the calcination temperature is reported.

Four pre-treatment temperatures were chosen for investigating the influence of the calcination step applied to the starting amorphous powder on its densification behaviour. Powder A was calcined at $600\,^{\circ}$C for 30 min, to maintain a fully amorphous product whereas powder B was treated at $800\,^{\circ}$C for 30 min, still to avoid crystallization and for limiting the residual weight loss, on the ground of the TGA results. Powder C was calcined at $900\,^{\circ}$C for 30 min to cause starting crystallization of h-$YAlO_3$, whereas powder D was treated at $1215\,^{\circ}$C for 0 h, to achieve fully crystallized YAG and traces of α-Al_2O_3. The XRD patterns of these four powders are compared in Fig. 3.

Firstly these materials were uniaxially pressed at 300 MPa and then sintered at $1600\,^{\circ}$C for 3 h in a dilatometer (Fig. 4). Green densities changed as function of the pre-
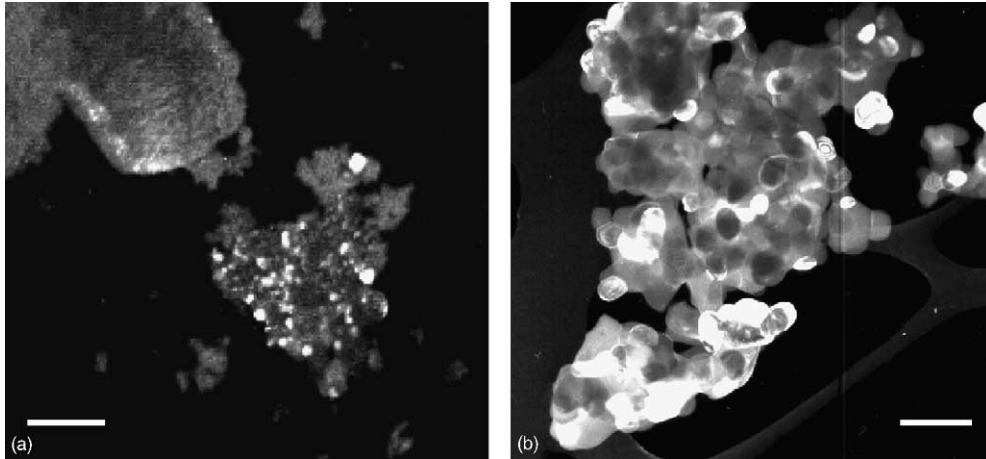
Fig. 1. (a) TEM analysis performed on AY50 powder head-treated at 900 °C for 30 min; bar = 300 nm (b) TEM analysis performed on AY50 powder head-treated at 1300 °C for 30 min; bar = 300 nm.
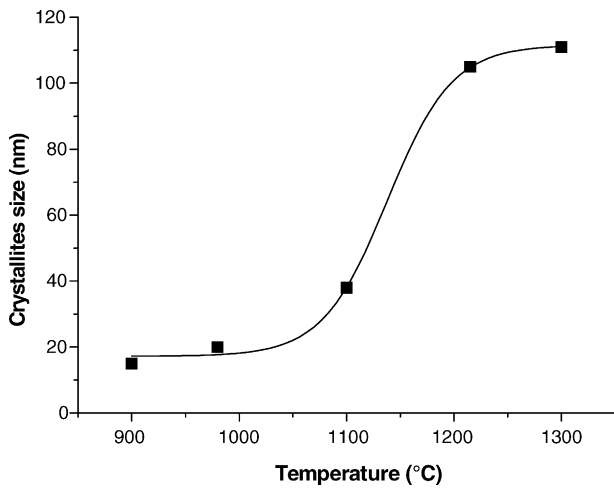
treatment temperature, precisely they ranged between 34.5 and 36.5% of the theoretical value ($4.25 \, g/cm^3$) for materials A, B and C, whereas it reached about 43% for sample D.

From the dilatometric curves, the onset densification temperatures for materials A and B are similar and very close to about 800 °C. The onset points of materials C and D are obviously affected by the higher pre-treatment temperatures. Except for the curve of material D, in which α-alumina is already partially formed, a large temperature step between about 1200 and 1550 °C, during which a strongly

Fig. 2. Crystallite size evolution as a function of the calcination temperature.

Fig. 3. XRD patterns as a function of the pre-treatment temperature; 600 °C for 30 min for sample (A); 800 °C for 30 min for sample (B); 900 °C for 30 min for sample C and 1215 °C for 0 h for sample D.
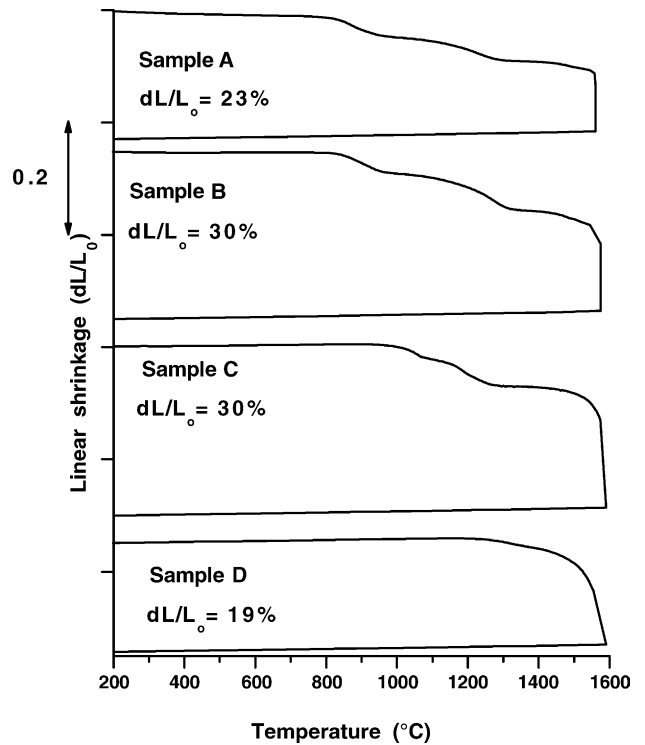

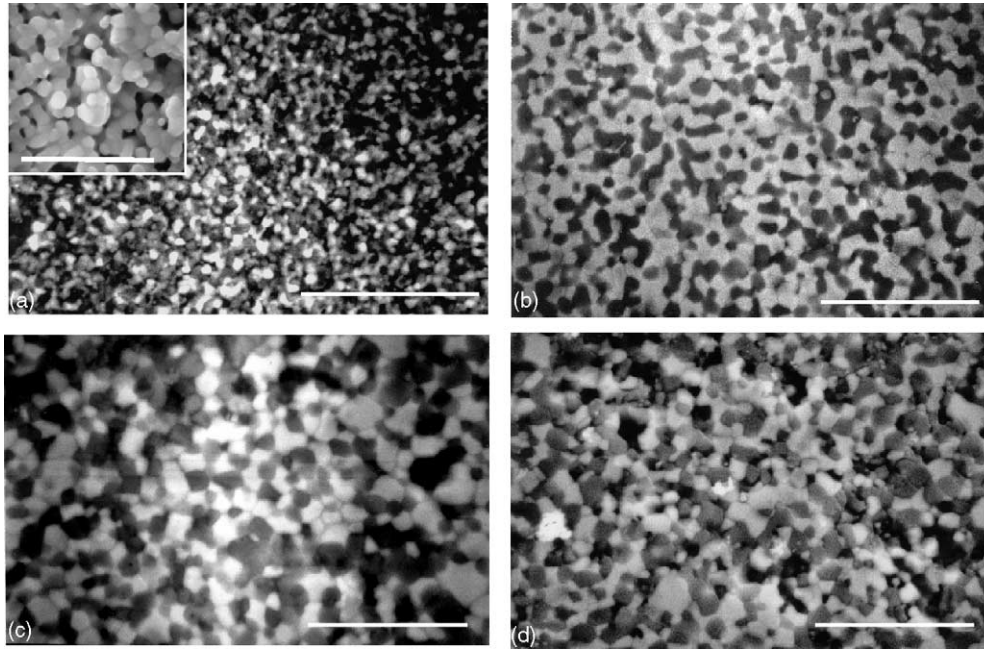Fig. 4. Dilatometric curves as a function of the pre-treatment temperature.

Fig. 5. BSE-SEM micrographs of the materials sintered at 1600 °C for 3 h: (a) sample A (in the insert a magnification showing a diffused porosity, bar = 5 μm); (b) sample B; (c) sample C; and (d) sample D. For all the images, bar = 10 μm.

limited shrinkage was observed, is linked to the crystallisation and growth of α-alumina grains from the transition phase. This step can be reasonably responsible for grain growth[19] without or with a limited, associated densification effect. This step must be therefore avoided to yield a final, dense nanostructure. A similar linear shrinkage (of about 30%) was observed in the samples B and C, whereas lower values, respectively 23 and 19%, were recorded in samples A and D.

In addition, the four materials showed different residual weight losses associated to the densification thermal cycle, namely 16%, 11.5%, 4.5% and 2% respectively for samples A, B, C and D.

Full densification (>99% of the theoretical value) was reached only by sample C, while samples A, B and D showed a final relative density of 65%, 90% and 80%, respectively. From SEM observations by using back-scattered electrons (BSE) (Fig. 5a–d), the microstructures are characterised by a highly homogeneous distribution of alumina and YAG grains. The mean grain size was about 1 μm in the samples B, C and D, whereas a value of about 0.6 μm was detected in sample A.

The low final density of the sample D could be imputed to the relevant lowering of the specific surface area of the powder, associated with the crystallization and growth of YAG and α-alumina. On the contrary, in sample A densification was limited by the weight loss (about 16%) associated with residual OH^- stripping from the amorphous precipitate, leading to a large, diffused residual porosity (see insert in Fig. 5a). In sample B this weight loss is reduced (about 11.5%), however, it still remained too high if compared to the values shown

by samples C and D, leading again to a large amount of entrapped porosity.

SEM analyses performed on MgO-doped samples did not reveal any relevant effect of the dopant in limiting grain growth in the case of the fully dense sample C as well as in improving final density for the other investigated samples.

Also the materials obtained by the powders pre-treated at 1290 °C, to develop both the final crystalline phases, showed very low final density ranging from 65 to 84%, this latter value been reached by the sample soaked for 15 min. Fast calcinations at 1290 °C, in fact, led to a phase development similar to that of the sample D, with a very well crystallized YAG with traces of α-alumina (Fig. 6).
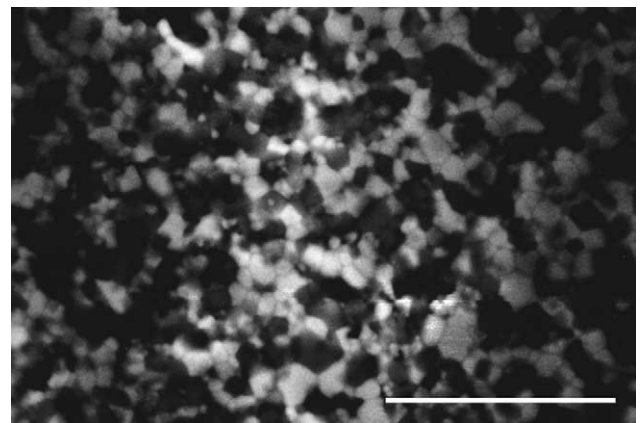

Fig. 6. BSE-SEM micrograph of the materials sintered at 1600 °C for 3 h, obtained by powders pre-treated at 1290 °C for 15 minutes. Bar = 10 μm.
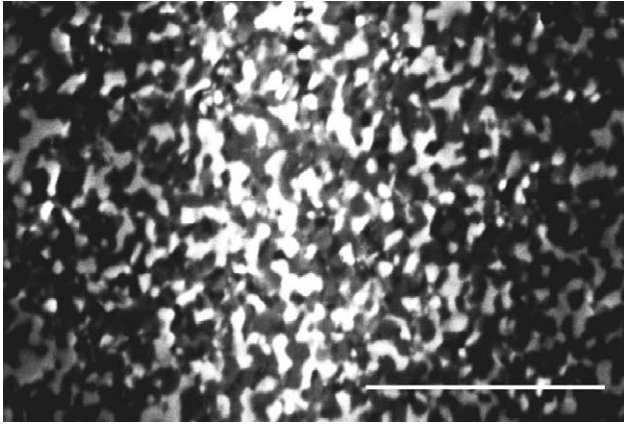
Fig. 7. BSE-SEM micrograph of the fast sintered material. Bar = 10 μm.

Concerning fast sintering, materials having a highly homogeneous distribution of the two phases with a mean grain size of about 500 nm were obtained, but once again a poor densification (60% of the theoretical density) was reached (Fig. 7). The two above negative results can be reasonably imputed to the difficulty of optimising a thermal cycle (in view of a partial pre-crystallization of the two final phases or even for densification) in a bi-phasic system in which the two phases are characterized by significantly different crystallization path and sinterability. More details on these previous attempts are reported elsewhere.[20]

Therefore, a mechanical activation by extensive milling was performed on the previously best performing sample, that is on material C. In Fig. 8 the first step of the dilatometric curves of material C just after calcination at 900 °C (curve a) and after mechanical activation (curve b) are compared. It clearly appears the strong effect of the milling step in displacing all the characteristic points to lower temperatures, including the onset densification temperature, the YAG as well as α-alumina crystallisation range and the maximum densification temperature. In fact, in the case of the activated material, a maximum temperature of 1420 °C was enough to achieve full densification.
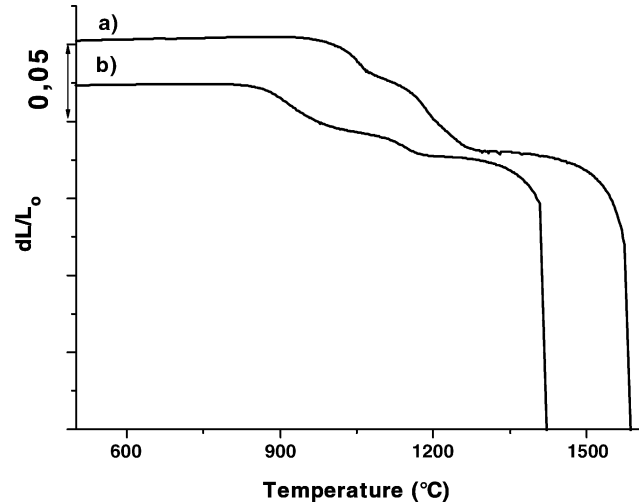

Fig. 8. Dilatometric curves of samples pre-treated at 900 °C for 30 min (a) before mechanical activation sintered at 1600 °C for 3 h and (b) after mechanical activation sintered at 1420 °C for 2 h.

In Fig. 9a (with a BSE image in the insert) and b the microstructures of the two sintered bodies are compared. In the case of the activated material (Fig. 9b), the microstructure was highly homogeneous and the grain size was very uniform and lower than 200 nm.

Since this mechanical activation step associated with an optimised thermal pre-treatment seems to offer good opportunities for nanostructured dense composites, the influence of the grinding media on the efficiency of the activation step was investigated.

Polyethylene, α-alumina and zirconia spheres having the same diameter were used for activating the 900 °C-pre-treated powder, by wet-milling for the same time. The impact energy of the grinding media plays a relevant role. To graduate this effect, bars were sintered at three different final temperatures, namely 1480, 1420 and 1370 °C. When sintered at 1480 °C, all the three powders fully densified, whereas at 1420 °C only the powders milled by using ceramic balls reached high density whereas the PE-milled material achieved just 75% of the theoretical density. At 1370 °C,
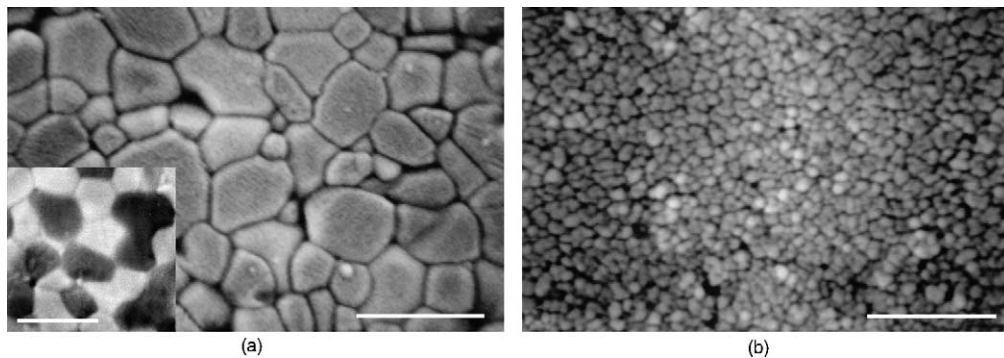

Fig. 9. SEM micrographs of sample C (a) before mechanical activation, sintered at 1600 °C for 3 h (bar = 2 μm). In the insert, a BSE SEM micrograph of the same sample is reported (bar = 2 μm); (b) SEM micrographs of sample C after mechanical activation and sintered at 1420 °C for 2 h; (bar = 2 μm).
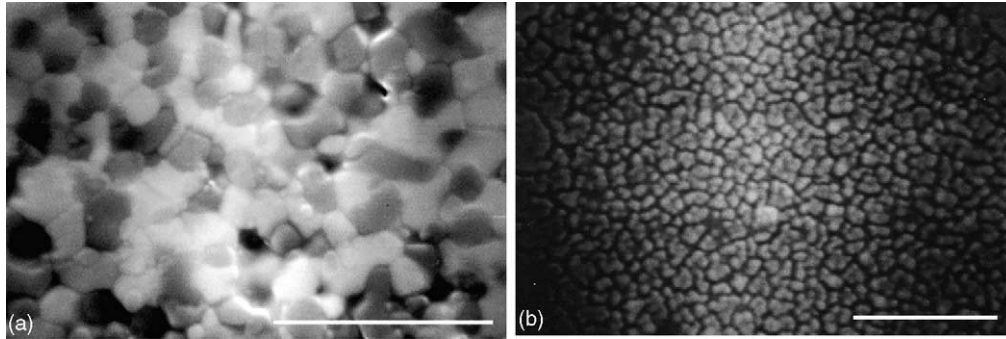
Fig. 10. Effect of zirconia ball milling: (a) BSE-SEM micrograph of the material sintered at 1420 °C for 2 h, bar = 5 μm and (b) SEM micrograph of the material sintered at 1370 °C for 3 h, bar = 2 μm.

both α-alumina and zirconia-milled materials reached quite full densification (>95% and 98% of the theoretical density, respectively) but the grain coarsening is affected by the nature of the grinding media. In fact, at a same sintering temperature (1420 °C), the materials milled by using α-alumina spheres presented a lower mean grain size (<200 nm) than the respective zirconia-milled materials (<1 μm) (Fig. 10a). A microstructure characterised by a mean grain size lower than 200 nm was obtained by sintering the zirconia-milled material at a lower temperature, namely 1370 °C (Fig. 10b).

Therefore, by combining the above sintering temperature, final density and mean grain size data, it clearly appears that in a very limited temperature range (from 1370 °C up to 1420 °C) the zirconia-milled material can evolve from a homogeneous nanostructure to a common microstructure. The activation parameters (time, milling media, etc.) must be therefore precisely set up to be successful in maintaining the desired structure level.

Since the mechanical activation has demonstrated to have a strong influence on the sinterability of these powders as well on the possibility to maintain a nanostructure, some other tests were performed on powders previously rejected (powders A and B). After extensive mechanical activation both materials reached a significant increase of final density (>90%) after sintering at 1420 °C for 2 h with a very fine microstructure comparable to that of powder C after activation, even if fully dense bodies were not yielded.

4. Conclusions

From the experimental results the following conclusions can be drawn out:

1. Thermal pre-treatment of the starting, amorphous powder is crucial in controlling the sinterability of these materials; the best results were obtained by using powders pre-treated at 900 °C for 30 min.
2. MgO showed a very limited effect as sintering aid in limiting grain coarsening during densification.
3. A thermal pre-treatment to induce a partial crystallization of the two final phases and a fast sintering procedure

were unsuccessful, probably due to the relevant difference in crystallization path and sinterability of the two final phases of this composite material. Anyway, these processes require further optimisation.
4. An alumina-YAG nano-nanocomposite material was yielded by coupling an optimised powder pre-treatment to an extensive mechanical activation, performed by a conventional wet (planetary + ball) milling. After that powder compacts fully sintered (>98%) at very low sintering temperature, ranging between 1370 and 1420 °C. As a consequence, a very fine microstructure was obtained in which α-alumina and YAG grains were lower than 200 nm in size.

References

1. Bowen, P. and Carry, C., From powders to sintered pieces: forming, transforming and sintering of nanostructured ceramic oxides. *Powder Technol.*, 2002, **128**, 248–255.
2. Seal, S., Kuiry, S. C., Georgieva, P. and Agarwal, A., Manufacturing nanocomposite parts: present status and future challenges. *MRS Bull.*, 2004, 16–21.
3. Stearns, L. C. and Harmer, M. P., Particle-inhibited grain growth in Al₂O₃-SiC: I. Experimental results. *J. Am. Ceram. Soc.*, 1996, **79**(12), 3013–3019.
4. Nordahl, C. S. and Messing, G. L., Sintering of α-Al₂O₃-seeded nanocrystalline γ-Al₂O₃ powders. *J. Eur. Ceram. Soc.*, 2002, **22**, 415–422.
5. Legros, C., Carry, C., Bowen, P. and Hofmann, H., Sintering of a transition alumina: effects of phase transformation, powder characteristics and thermal cycle. *J. Eur. Ceram. Soc.*, 1999, **19**, 1967–1978.
6. Chen, I.-W. and Wang, X.-H., Sintering dense nanocrystalline ceramics without final-stage grain growth. *Nature*, 2000, 168–171.
7. Harmer, M. P., Roberts, E. W. and Brook, R. J., Rapid sintering of pure and doped α-Al₂O₃. *Trans. J. Br. Ceram. Soc.*, 1979, **78**, 22–25.
8. Garcia, D. E., Seidel, J., Janssen, R. and Claussen, N., Fast firing of alumina. *J. Eur. Ceram. Soc.*, 1995, **15**, 935–938.

9. Palkar, V. R., Thapa, D., Multani, M. S. and Malghan, S. G., Densification of nanostructurated alumina assisted by rapid nucleation of α-alumina. *Mater. Lett.*, 1998, **36**, 235–239.

10. Kuntz, J. D., Zhan, G.-D. and Mukherjee, A. K., Nanocrystalline-matrix ceramic composites for improved fracture toughness. *MRS Bull.*, 2004, 22–27.

11. Gao, L., Shen, Z., Miyamoto, H. and Nygren, M., Superfast densification of oxide/oxide ceramic composites. *J. Am. Ceram. Soc.*, 1999, **82**(4), 1061–1063.

12. Apte, P., Burke, H. and Pickup, H., Synthesis of yttrium aluminum garnet by reverse strike precipitation. *J. Mater. Res.*, 1992, **7**(3), 706–711.

13. Li, J. G., Ikegami, T., Lee, J. H., Mori, T. and Yajima, Y., Co-precipitation synthesis and sintering of yttrium aluminum garnet (YAG) powders: the effect of precipitant. *J. Eur. Ceram. Soc.*, 2000, **20**, 2395–2405.

14. Wang, H., Gao, L. and Niihara, K., Synthesis of nanoscaled yttrium aluminum garnet powder by the Co-precipitation method. *Mater. Sci. Eng.*, 2000, **A288**, 1–4.

15. Bennison, S. J. and Harmer, M. P., Effect of MgO solute on the kinetics of grain growth in Al_2O_3. *J. Am. Ceram. Soc.*, 1983, **65**(5), C90–C92.

16. Wang, J., Lim, S. Y., Ng, S. C., Chew, C. H. and Gan, L. M., Dramatic effect of a small amount of MgO addition on the sintering of Al_2O_3–5 vol.% SiC nanocomposite. *Mater. Lett.*, 1998, **33**, 273–277.

17. Palmero, P, Simone, A., Stella, C. and Montanaro, L., Inventor's Italian Patent No. TO2004A000453.

18. Yamaguchi, O., Takeoka, K., Hirota, K., Takano, H. and Hayashida, A., Formation of alkoxy-derived yttrium aluminium oxides. *J. Mater. Sci.*, 1992, **27**, 1261–1264.

19. Dynys, F. W. and Halloran, J. W., Alpha alumina formation in alum-derived gamma alumina. *J. Am. Ceram. Soc.*, 1982, **65**(9), 442–448.

20. Palmero, P., Simone, A. and Stella, C., Influence of some processing parameters on the production of fully dense nanocomposites materials. In *Proceedings of CIEC 9, 9th European Interregional Conference of Ceramics, Bardonecchia, Italy, 5–7 September 2004*. eds. A. Negro and L. Montanaro, Politecnico di Torino, Italy, pp. 173–178.